Ku Band Backscatter from the Cowlitz River: Bragg scattering with and without rain

Robert F. Contreras
Department of Atmospheric Sciences
University of Washington
Seattle, Washington

William J. Plant
Applied Physics Laboratory
University of Washington
Seattle, Washington

February 18, 2004

Abstract

Ku band backscatter from the Cowlitz River in southwestern Washington State was measured for incidence angles from 0° to 80°. The measurements were made for light-wind conditions with and without rain. In rain-free conditions, Bragg scattering was the dominant scattering mechanism for both HH and VV polarizations out to 75°, beyond which the signal-noise-ratio dropped very low at HH. When a light rain was falling on the river, the cross section increased substantially at moderate incidence angles. Doppler spectra taken during rain showed that VV polarized backscatter is primarily from Bragg scattering from ring waves while HH polarization scatters from both ring waves and stationary splash products, depending on the incidence angle. From the VV polarized measurements a surface wave height spectrum for ring waves is inferred for light rains. Finally, a change in spectral properties was observed when rain changed to hail.

1 Introduction

Microwave backscatter from the ocean and in wind-wave tanks has been investigated for many years, but backscatter from rivers has only recently received attention (Costa et al., 2000). Microwave backscatter from the ocean is used to probe the state of the ocean surface. Synthetic aperture radars (SARs) give high resolution images of surface roughness in which atmospheric as well as oceanic phenomena are visible. Altimeters use the time of travel of backscatter to determine ocean surface height. Scatterometers use backscatter to infer vector winds at the surface. Understanding the scattering mechanisms responsible for backscatter enables us to correctly interpret the backscattered signals and relate them to physical phenomena. At very low incidence angles (close to nadir) quasi-specular reflection approximates the backscatter rather well and the mean square slope of the surface determines the backscattered radiation.

As the incidence angle moves away from nadir, backscatter must be explained by a Kirchoff integral formulation, which becomes well approximated by Bragg scattering as the incidence angle increases. Bragg scattering is a resonance condition in which radiation incident upon identical phases of a surface wave has a phase difference of half a wavelength of the radiation; the returning radiation is then a full wavelength out of phase, or precisely in phase. When this condition is met the backscatter is much stronger than predicted by quasi-specular scattering. This scattering mechanism rapidly becomes important when moving off nadir. At a 10° incidence angle, Bragg scattering makes up greater than about 50% of the total backscatter from the ocean for wind speeds less than 5 m s^{-1} (Plant, 2002). At 30°, virtually all of the backscatter is due to Bragg scattering. As discussed in Plant (1997, 2003a), at high incidence angles ocean backscatter differs from the predictions of Bragg scattering as augmented by standard composite surface theory. The main differences are that HH polarized backscatter is more intense than predicted and has larger Doppler shifts. These anomalies have been explained in two primary ways. One is that Bragg theory is still applicable but free and bound, tilted waves need to be considered in scattering calculations (Plant, 1997, 2002, 2003b). The other is that scattering mechanisms other than Bragg need to be considered (Lee et al., 1999; West and Ja, 2002), especially at very high incidence angles (or very low grazing angles). The concept of "fast scatterers" has been suggested to combine these effects. The idea is that HH polarized backscatter is from fast moving features of breaking waves. This does not exclude the possibility of Bragg scattering but at the highest incidence angles (or lowest grazing angles) where multiple scattering, shadowing, and scattering from sharp peaks must also be considered. Signatures of bound waves have also been shown in Plant et al. (1999) and Plant (2003b) to be present in slope probability density functions (PDFs) both in the laboratory and on the ocean. In backscatter in laboratory wind-wave tanks, bound waves are often the primary scatterers at both polarizations (Plant et al., 1999); on the ocean they are the primary scatterers only at HH polarization at large incidence angles (Plant, 1997). Accurately determining the mechanism by which microwave radiation is backscattered from the ocean has been difficult because of the wide range of wave scales present. In addition to the incompletely understood dynamics of the small wave field, larger waves generate, tilt, and advect the smaller waves, making it difficult to associate backscatter with specific short wave features. The study presented here shows that backscatter is simpler at low wind speeds on moderately turbulent rivers, where very long waves are absent, and that this simplicity allows the investigation of high incidence angle backscatter and the effects of rain on rough surface backscatter.

During rain, Ku band cross sections at moderate to large incidence angles are enhanced (Hansen, 1986; Bliven et al., 1997; Sobieski et al., 1999; Lemaire et al., 2002; Braun, 2002; Contreras et al., 2003). This is due to the creation of scattering features by impinging raindrops. The splash associated with a raindrop impinging on the water starts with a crater and crown which collapse to form a stalk. Following this, ring waves propagate radially outward. Photographs of this phenomena were first taken by Worthington (1963). Many wave tank studies have been conducted to attempt to determine which of these splash products are the primary scatterers of microwaves. Hansen (1986) and Sobieski et al. (1999) synchonized centimeter (0.8 to 3.3 cm) wavelength microwave backscatter measurements to video and high speed photography and determined the relative contributions of different splash products. From his studies Hansen (1986) decided that HH polarization scattered primarily from the stalk and VV polarization from all splash features over his range of incidence angles, 8° to 45°. Sobieski

et al. (1999) concluded that ring waves are primarily responsible for the increased backscatter, although the contribution from the stalk is non-negligible. Braun (2002) showed that backscatter from different splash products is dependent on incidence angle and polarization. By observing Doppler spectra, she concluded that VV polarization backscatters from ring waves while HH polarization backscatters from ring waves at low incidence angles and stationary splash products at high angles. She observed the incidence angles: 29°, 40°, and 55°. At angles where ring waves dominated, Bragg scattering was the scattering mechanism, as evidenced by two peaks that appear in the Doppler spectra. The peaks correspond to Bragg resonant waves traveling away from and toward the antenna. The two peaks occurred in HH polarization data at low to moderate incidence angles but at large incidence angles, a third peak appeared at zero frequency. This indicated a contribution from stationary splash products, such as the crown and stalk, which eventually dominated the total return. Except for Smith et al. (1998) who studied the effect of rain on S band backscatter, which has a much longer wavelength, all of the rain studies identifying relative backscatter from splash products have been done in the laboratory with artificial rain.

In this paper, measurements will be presented of backscatter from the Cowlitz River in southwestern Washington State during both raining and non-raining conditions. The data will show that backscatter from the river is Bragg scattering at moderate to large incidence angles during non-raining conditions. This will be shown to be true out to incidence angles of 75°, much farther than Bragg scattering has been thought to apply on the ocean. The measurements will also show that a light natural rain increases backscatter at moderate to large incidence angles, in agreement with our work at sea (Contreras et al., 2003). Doppler spectra will show that VV backscatter during rain is due to ring waves while HH backscatter is from ring waves at moderate incidence angles but contains substantial contributions from stationary splash products at high incidence angles. The response of VV backscatter to ring waves will allow us to determine their spectral properties from the backscatter.

2 Ku Band River Measurements

During winter and spring 2003, measurements of Ku band backscatter were made from a bridge spanning the Cowlitz River at Castle Rock in southwestern Washington State. Measurements were made at incidence angles from 0° to 80° at a height of roughly 11 meters above the water surface. Wind measurements were made coincident with the backscatter measurements, as were measurements of rain rate, rain drop size distribution, river gage height, and surface velocity. The microwave system was a dual polarized continuous wave (CW) coherent system operating at 14 GHz (Ku band). The antenna full, two-way, half-power beamwith is 4.8 degrees. The backscatter is represented as the normalized radar cross section σ_o. Since the system is coherent, Doppler spectra of the backscatter were computed, which allowed the identification of backscattering features. A further discription of the system and the calculation of cross section can be found in Contreras et al. (2003). The sample rate is 2048 Hz and spectra were computed each second. Sixty spectra make up the basic sample shown here, providing one minute average spectra. Cross sections were also computed as one minute averages.

The rain rate and drop size distributions were measured using a Joss-Waldvogel disdrometer located atop a USGS shed roughly 60 meters from the CW system. Wind measurements

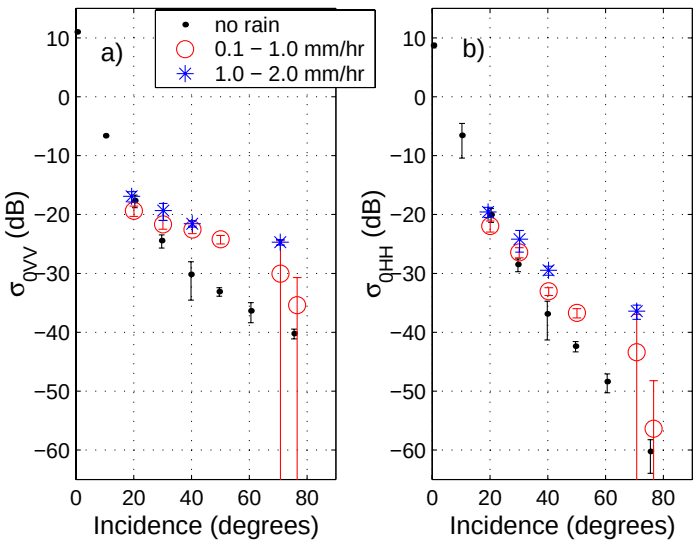

Figure 1: Cross section as a function of incidence angle for wind speeds between 1 and 3 m s^{-1} within 45° of the downwind direction.

were also made at the shed.

The antenna looked upriver (north) in order to avoid measuring backscatter from features created in the turbulent wake downstream of the bridge supports. During rain, the wind was predominately from the south, so data presented here are within 45° of the downwind azimuth angle. Fig. 1 is an example of the observations that were made showing VV and HH polarized cross sections measured during rain free and light rain conditions when the wind was light.

3 Bragg Scattering

The panels of Fig. 2 show mean Doppler spectra of VV and HH polarized backscatter measured over the range of incidence angles from 0° to 75° in rain-free conditions. These spectra correspond to the non-raining data shown in Fig. 1. In rain-free conditions HH polarized cross sections were in the noise when the incidence angle was 80°, so data were only used out to 75°. The mean Doppler spectra are comprised of spectra which are centered on the first moment of VV polarized backscatter thereby removing the Doppler shifts due to mean surface motions. This allowed spectra measured at different times under different flow conditions to be compared. The widths of the spectra broadened with incidence angle from 7 Hz at nadir to 31 Hz at 75° and were insensitive to the wind speed. Only a single peak was observed in the spectrum since the antenna looked nearly downwind and the upwind-travelling wind-wave was very weak. The widths can be used to estimate the variations of surface velocities in the horizontal and vertical directions. Since the widths were independent of the wind speed, unlike the cross sections and magnitude of the spectra, the entire data set when it was not raining was used to determine the velocity variations. This differs from the cross sections and spectra shown in Fig. 1 and Fig. 2 which were for limited wind speeds and directions. The standard de-

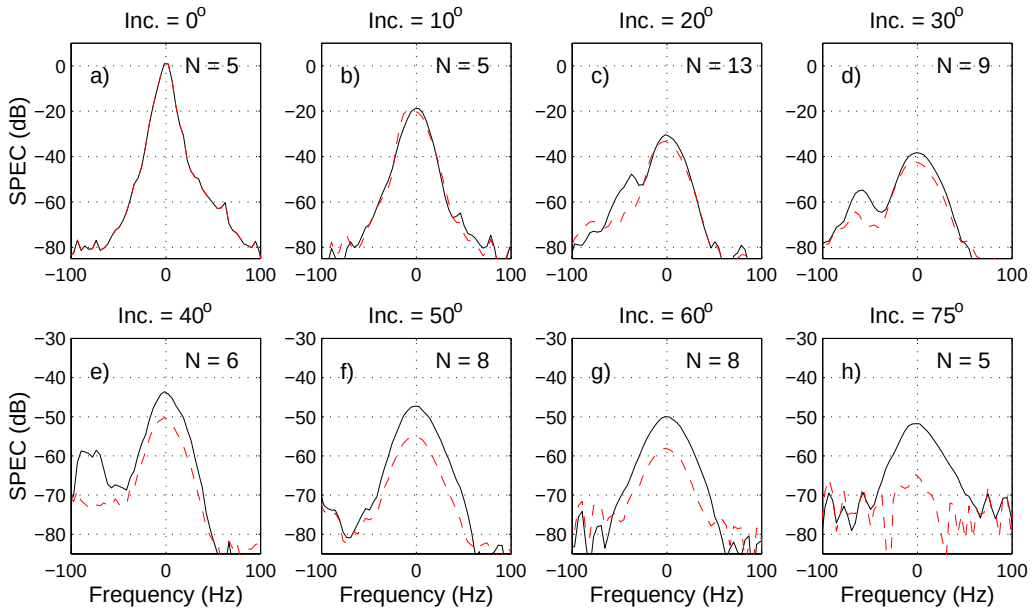

Figure 2: Doppler spectra of VV (solid) and HH (dashed) polarization backscatter during rain free conditions over the range of incidence angles: a) 0°, b) 10°, c) 20°, d) 30°, e) 40°, f) 50°, g) 60° and h) 75°. The wind was within 45° of the downwind direction with a magnitude between 1 and 3 m s^{-1}. The number of one minute samples going into the mean is indicated by N.

viation of the horizontal velocity was 17 $\pm$ 2 cm s^{-1}. The mean horizontal current which was roughly 1.7 m s^{-1} gave a contribution to the Doppler width at nadir due to antenna beamwidth. This contribution was 4 cm s^{-1} and it was the dominant source of the spectral width at nadir suggesting variations in vertical velocities were very small. As mentioned above, the variance in horizontal surface velocity was independent of wind speed, which indicates that wind is not driving the larger scale surface motions. It is reasonable to expect that the variances would be dependent on quantities relating to the flow such as the surface flow speed or the gage height. However, when these data were obtained the gage height was between 10.5 m (34.5 ft) and 11.1 m (36.5 ft) and the surfaces velocities were moderate; the mean flow did not change much. On the ocean, the widths of the spectra are the same at different incidence angles because the surface velocity variations are dominated by surface waves with circular orbital velocities, and thus equivalent horizontal and vertical velocity variations. Widths of ocean Doppler spectra are usually considerably larger than those shown in Fig. 2, being on the order of 100 Hz, corresponding to rms velocities of about 30 cm/s (Plant et al., 1994). The secondary peaks noticeable at negative Doppler frequencies at 20°, 30° and 40° incidence angles are probably from antenna sidelobes. They have been removed from the cross sections and should be disregarded. In any case, the largest is 15 dB below the spectral peak.

Fig. 3a shows mean VV and HH polarized cross sections when the wind speed is between 1 and 3 m s^{-1} looking downwind. In the figure symbols are data: VV polarization (dots) and HH polarization (circles). The solid line is the prediction of HH polarization using Bragg theory and VV cross sections. Fig. 3b shows the corresponding ratios of VV polarized cross sections

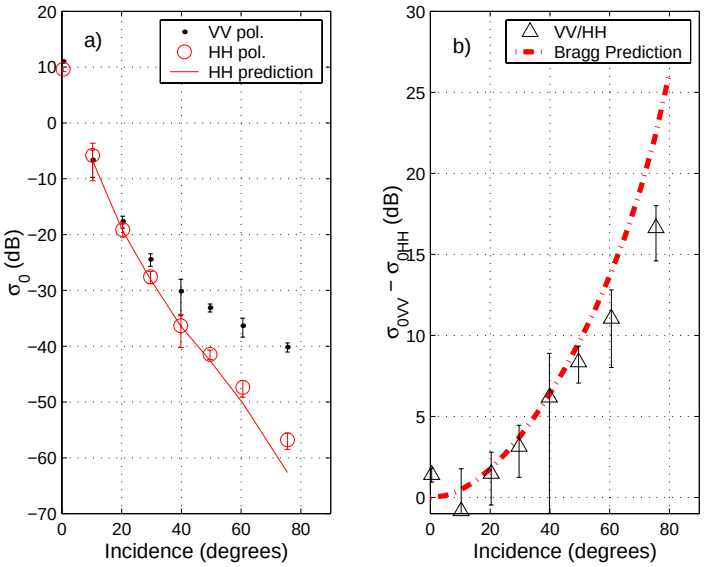

Figure 3: a) Cross section as a function of incidence angle for wind speeds between 1 and 3 m s^{-1} relative to the water surface. The symbols are data: VV polarization (dots) and HH polarization (circles), and the solid line is the prediction of HH polarization using Bragg theory and VV cross sections. b) Ratio of VV polarization to HH polarization (triangles) and the ratio predicted by Bragg scattering (dash-dot). Errorbars signify the 95% confidence interval.

to HH polarized ones. For standard Bragg/composite surface scattering, the polarization ratio is independent of the surface wave spectrum and is only a function of the incidence angle. The polarization ratio predicted by Bragg scattering is the dash-dotted line in the figure. Although the standard error is relatively large, all of the means fall close to the prediction of Bragg scattering indicating that it is the dominate source of backscatter at moderate and high incidence angles. Also the similarity of HH and VV Doppler spectra suggest that the same surface waves or features are responsible for the backscatter. This is in contrast with ocean backscatter for which HH polarized backscatter at large incidence angles has a significant component from bound, tilted waves with Doppler shifts much greater than the intrinsic phase speeds of the Bragg resonance waves. This causes HH Doppler spectra on the ocean to appear at higher frequencies than VV spectra at high incidence angles (Plant, 1997).

4 Scattering During Rain

Rain significantly increases Ku band backscatter at moderate and high incidence angles. Fig. 1 shows the effect of light rain on the cross section. For light winds and a rain rate between 0.1 and 1.0 mm hr^{-1}, backscatter at 20° was relatively unchanged, while it increased by roughly 10 dB at 50°. The changes for rainfall rates between 1.0 and 2.0 mm hr^{-1} were even greater. Evidence for Bragg scattering from the river surface was observed during rain. When rain is falling, the Doppler spectra show two peaks corresponding to ring waves traveling toward and away from the antenna, giving a separation corresponding to twice their phase

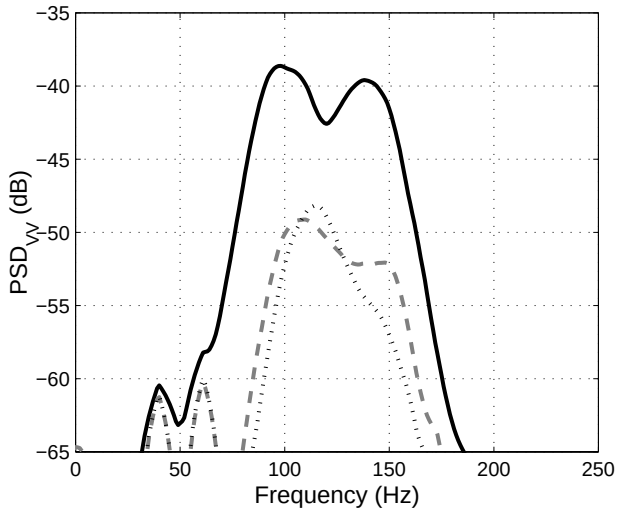

Figure 4: Three consecutive one minute average VV polarizaton Doppler spectra at the cessation of rain at an incidence angle of 71°. Rainfall rates are 2.8 mm hr^{-1} (solid), 0.4 mm hr^{-1} (dashed), and 0.0 mm hr^{-1} (dotted).

speed. Strong backscatter from both waves is expected since the spectral densities of waves traveling in both directions are the same and they dominate wind-generated waves. Fig. 4 shows VV polarized Doppler spectra as the rainfall rate changed from 2.8 mm hr^{-1} (solid) to 0.4 mm hr^{-1} (dashed) to 0.0 mm hr^{-1} (dotted). At this time the antenna looked in the downwind direction and the wind speed was about 3.5 m s^{-1} relative to the river surface. The two peaks clearly noticeable during the 2.8 mm hr^{-1} rain correspond to backscatter from ring waves. As the rain decreased to 0.4 mm hr^{-1} the cross section decreased significantly, from -22.0 dB to -33.9 dB. This decrease in backscatter was a result of the decrease in the spectral density of ring waves associated with smaller and fewer drops during the lighter rain. There were, however, two peaks in the Doppler spectrum at this light rainfall rate and they were similarly separated by a frequency interval corresponding to waves traveling away from each other. The shift to higher frequencies suggests variations in the mean surface velocities of the river while the asymmetry of the peak heights shows that wind waves are beginning to be seen in addition to ring waves. Finally, the spectrum observed with no rain falling consisted of a single Doppler peak corresponding to backscatter associated with wind-generated waves. The asymmetry in the spectrum at about 150 Hz is typical of backscatter from wind waves propagating nearly along the horizontal antenna look direction and was the result of backscatter from the much weaker Bragg-resonant wave traveling opposite the wind direction. The total cross section in this non-raining case was -35.0 dB.

Unlike river backscatter for non-raining conditions, VV polarization and HH polarization scatter from different surface features during rain at high incidence angles. Fig. 5 shows average VV and HH polarized spectra during rain between 0.1 and 1.0 mm hr^{-1}. Like those shown in Fig. 2, the spectra going into these averages have had the first moment of VV polarized backscatter removed to eliminate differences in the mean flow velocities between individual records. The separation of the two Bragg peaks is consistent with ring waves traveling toward

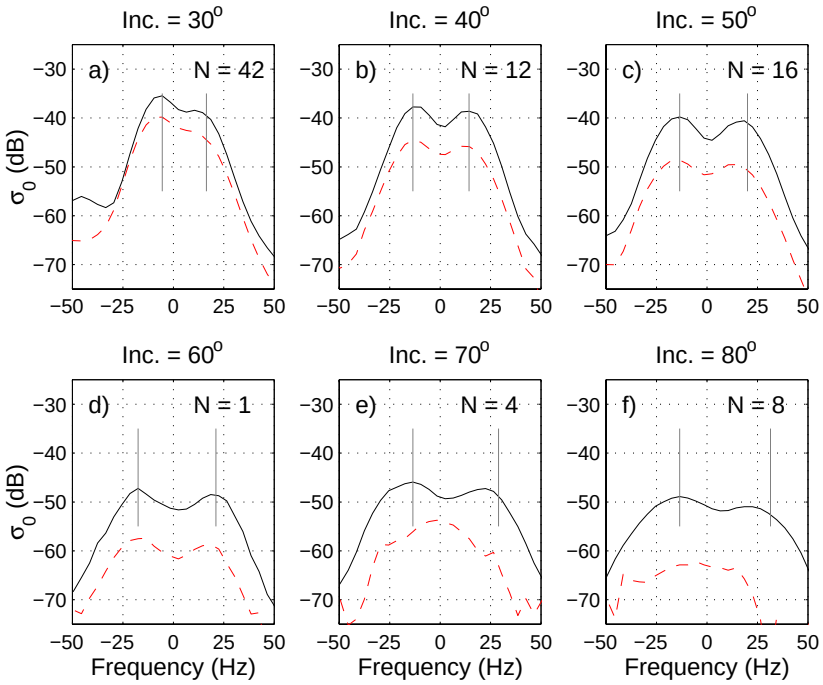

Figure 5: Doppler spectra of VV (solid) and HH (dashed) polarized backscatter during rainfall of 0.1 to 1.0 mm hr^{-1} at the following incidence angles: a) 30°, b) 40°, c) 50°, d) 60°, e) 70° and f) 80°. The separation of Doppler peaks expected from ring waves traveling toward and away from the antenna are shown as gray lines with the left line at the maximum of the first peak. The wind was within 45° of the downwind direction and the wind speed was 1 and 3 m s^{-1}. The number of one minute samples going into the mean is indicated by N.

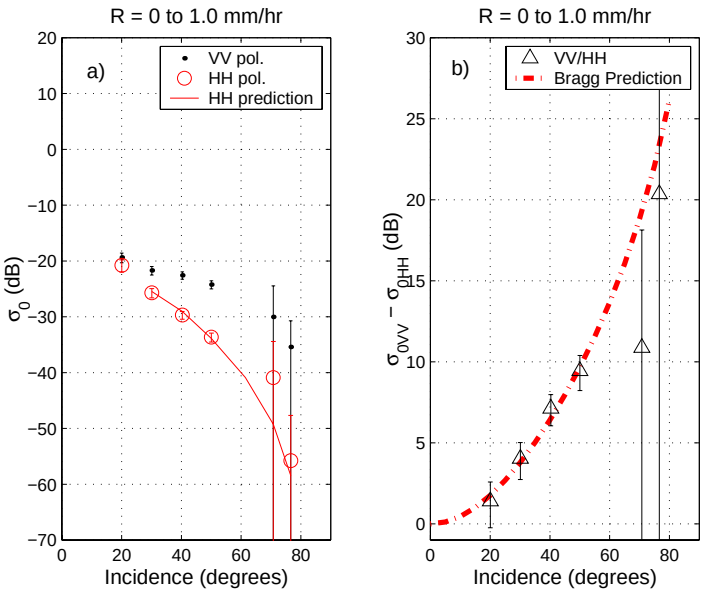

Figure 6: a) Cross section as a function of incidence angle for water surface relative wind speeds between 1 and 3 m s^{-1} for rainfall rates between 0.1 and 1.0 mm hr^{-1}. The symbols are data: VV polarization (dots) and HH polarization (circles), and the solid line is the prediction of HH polarization using Bragg theory and VV cross sections. b) Ratio of VV polarization to HH polarization (triangles) and the ratio predicted by Bragg scattering (dash-dot). Errorbars signify the 95% confidence interval.

and away from the antenna and can be seen in all the VV polarized spectra. The separation of Doppler peaks expected from ring waves traveling toward and away from the antenna are shown as gray lines with the left line at the maximum of the first peak. At 70° and 80° the separation is less than expected which has the likely explanation that the contribution from the stationary splash products is becoming significant and acting to bias the spectral peaks toward the Doppler shift associated with stationary surface features. Note that the distance between the peaks is much larger than the width of the peak seen during non-raining conditions. This confirms our assessment that the non-raining spectrum was a single Bragg peak. In the HH polarized spectra the ring wave backscatter is noticeable out to 60°. At 70° the cross section was dominated by backscatter from stationary features of the splash. Fig. 6a shows σ_o during a light rain between 0.1 and 1.0 mm hr^{-1} as a function of incidence angle. Fig. 6b shows the polarization ratio of the data and of that predicted by Bragg scattering.

5 Onset of Hail

The effect of hail on Ku band backscatter was also observed. Fig. 7a shows Doppler spectra during rain of 12.4 mm hr^{-1} at an incidence angle of 71°. Centered at about -600 Hz is the backscatter associated with the falling raindrops. At about 150 Hz, backscatter from the water surface is visible. The VV polarized spectrum shows the double peaks due to ring waves while

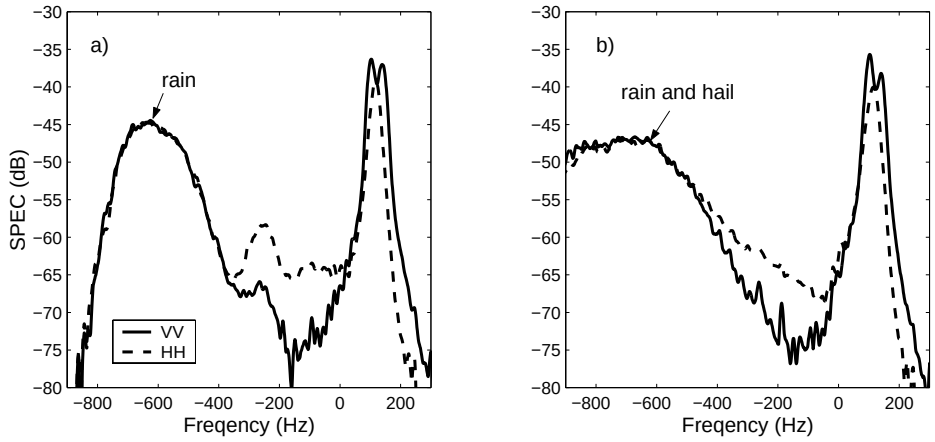

Figure 7: VV (solid) and HH (dashed) polarization Doppler spectra for a) rain and b) rain and hail.

the HH polarized spectrum shows a single peak from stationary splash products. During the next minute (Fig. 7b) hail began to fall. The cross sections from the hydrometeors remained relatively the same: VV polarization stayed at -22 dB and HH polarization went from -21 to -22 dB. The most dramatic change occurred in the Doppler spectra of the backscatter from the hydrometeors which shifted to lower frequencies and significantly broadened, indicating greater fall velocities and much greater variance in the fall velocities. Considering wind speed and direction at the time, the fall velocity of the hydrometeors increased from 5 m s^{-1} to 8 m s^{-1} and the standard deviation of the fall speed increased from roughly 2 m s^{-1} to 4 m s^{-1}. With the onset of hail, VV polarized surface backscatter went from -19 to -20 dB and HH polarized ones stayed constant at -25 dB. In both cases, VV polarized spectra showed two Bragg peaks corresponding to rings waves. Although, the higher frequency ring wave peak decreased relative its counterpart in hail-free conditions, the limited number of samples and the modest change during hail make it difficult to draw any conclusions about changes in the scattering surface features. HH polarization surface spectra show a single peak with little change during hail.

6 Ring Wave Model

Since our data indicate that ring waves are the dominate scatterers of VV polarized backscatter during rainfall and that Bragg scattering is the scattering mechanism, the change in cross section during rain can be inverted and the wave height variance spectrum of the ring waves determined. The inversion of backscatter to the surface spectrum is expressed as

$$F = \frac{1}{16\pi k_o^4} \frac{\sigma_o}{|g_{qp}|^2} \tag{1}$$

where F is the folded wave height variance spectrum, k_o is the wavenumber of the transmitted radiation and g_{qp} is a function taking into consideration the geometry, dielectric properties of water and the polarization of the radiation. These functions can be found as Eq. 2 and 3 in Plant (2002). Since ring waves are isotropic and dominate the short wave field, the backscatter

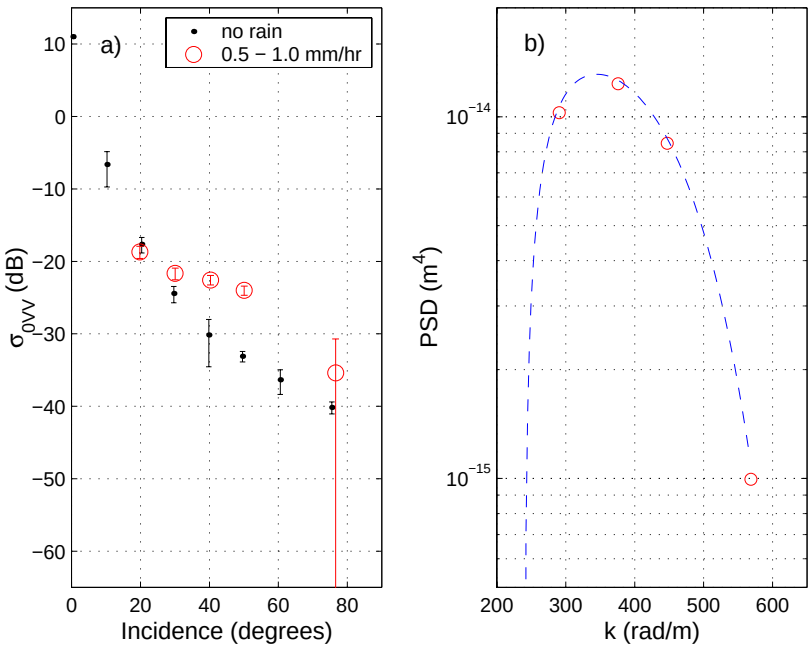

Figure 8: a) Cross section as a function of incidence angle for water surface relative wind speeds between 1 and 3 m s^{-1} for no rain (dots) and rain between 0.5 and 1.0 mm hr^{-1} (circles). b) Ring wave surface height variance spectrum inferred from a).

is independent of azimuth angle. Fig. 8a shows the backscatter associated with a rainfall rate of 0.5 to 1.0 mm hr^{-1}. Fig. 8b shows the ring wave spectrum determined from inverting the change in cross section between non-raining and raining conditions. This assumes that the combined spectrum can be considered the sum of a wind-driven spectrum and a rain-only spectrum. This assumption is reasonable at incidence angles where rain backscatter dominates the total backscatter but becomes weaker at lower incidence angles where the cross sections from the two sources are comparable and rain drops impinging upon the surface probably affect the wind waves. At 70° there was no non-raining data so the difference between rain-created and wind-created backscatter could not be assessed; the highest wavenumber represented was roughly 570 rad m^{-1} at an incidence angle of 75°. The ring wave spectrum has a maximum between 300 and 400 rad m^{-1} which corresponds to surface waves slightly less than 2 cm, roughly where the surface wave phase speed reaches its minimum.

7 Discusion

During light-wind, non-raining conditions polarization ratios support the idea that Bragg scattering is the primary mechanism responsible for Ku band backscatter from the river over a wide range of incidence angles. The single peak in the spectra is evidence that the backscatter is from Bragg resonant waves traveling with the wind.

When rain is falling, VV and HH polarized backscatter both increase at moderate to large

incidence angles. VV polarized backscatter is primarily from ring waves at all incidence angles greater than about 20°. HH polarized backscatter is primarily from ring waves from 20° to 60°, above this stationary splash products, such as the crown and stalk, begin to affect the backscatter. This result is consistent with laboratory studies presented by Braun et al. (1999), although HH polarized ring-wave backscatter is observed here at greater incidence angles.

The differences between the ocean and the Cowlitz River also need to be addressed. The ocean is saline while the river is not. Sobieski et al. (1999) and Craeye et al. (1999) have shown that the characteristics of the splash products are insensitive to the salinity of the water surface. Therefore, salinity is a minor effect when considering the difference between river and ocean surface wave spectra at the scale of ring waves. It should be emphasized that the interactions between the rain and larger scale waves and turbulence are not considered here and comparisons to the ocean should not be drawn beyond the scale of ring waves. The most dramatic difference between a river and the ocean, of course, is the much longer wave scales found on the ocean. For the purpose of studying Bragg scattering and the scattering from splash products, this difference is important and working on a river has allowed us to ignore the effects of large waves and has enabled us to identify the primary scattering features. Differences between Bragg scattering on a river and on the ocean are probably due to properties of the ocean such as long waves and spray that are not easy to identify or include in basic scattering models.

8 Acknowledgments

The authors would like to acknowledge the contributions of Jeff Nystuen, Chris Siani, Bill Keller, and Ken Hayes to this research. The study was funded by the Office of Naval Research under grant numbers N00014-97-1-0708 and N00014-00-1-0075.

References

Bliven, L. F., P. W. Sobieski and C. Craeye, 1997: Rain generated ring-waves: Measurement and modeling for remote sensing. *Int. J. Remote Sens.*, **18**(1), 221–228.

Braun, N., 2002: *Untersuchungen zur Radar-Rückstreuung und Wellendämpfung beregneter Wasseroberflächen*. Ph.D. thesis, Univesität Hamburg.

Braun, N., M. Gade and P. A. Lange, 1999: Radar backscattering measurements of artificial rain impinging on a water surface at different wind speeds. in *IEEE 1999 International Geoscience and Remote Sensing Symposium (IGARSS)*, Vol. 1, pp. 200–202.

Contreras, R. F., W. J. Plant, W. C. Keller, K. Hayes and J. Nystuen, 2003: Effects of rain on Ku band backscatter from the ocean. *J. Geophys. Res.*, **108**(C5), 3165, doi:10.1029/2001JC001255.

Costa, J. E., K. R. Spicer, R. T. Cheng, F. P. Haeni, N. B. Melcher, E. M. Thurman, W. J. Plant and W. C. Keller, 2000: Measuring stream discharge by non-contact methods: A proof-of-concept experiment. *Geophys. Res. Lett.*, **27**(4), 553–556.

Craeye, C., P. W. Sobieski, L. F. Bliven and A. Guissard, 1999: Ring-waves generated by water drops impacting on water surfaces at rest. *IEEE J. Oceanic Eng.*, **24**(3), 323–332.

Hansen, J. P., 1986: Rain backscatter tests dispel old theories. *Microwaves and RF*, **6**, 97–102.

Lee, P. H. Y., J. D. Barter, K. L. Beach, B. M. Lake, H. Rungaldier, H. R. T. Jr., L. Wang and R. Yee, 1999: What are the mechanisms for non-Bragg scattering from water surfaces? *Radio Sci.*, **34**(1), 123–138.

Lemaire, D., L. F. Bliven, C. Craeye and P. Sobieski, 2002: Drop size effects on rain-generated ring-waves with a view to remote sensing applications. *Int. J. Remote Sens.*, **23**(12), 2345–2357.

Plant, W. J., 1997: A model for microwave Doppler sea return at high incidence angles: Bragg scattering from bound, tilted waves. *J. Geophys. Res.*, **102**(C9), 21,131–21,146.

Plant, W. J., 2002: A stochastic, multiscale model of microwave backscatter from the ocean. *J. Geophys. Res.*, **107**(C9), 3120, doi:10.1029/2001JC000909.

Plant, W. J., 2003a: Microwave sea return at moderate to high incidence angles. *Waves in Random Media*, **13**(4), 339–354, doi: 10.1088/0959-7174/13/4/009.

Plant, W. J., 2003b: A new interpretation of sea-surface slope probability density functions. *J. Geophys. Res.*, **108**(C9), 3295, doi:10.1029/2003JC001870.

Plant, W. J., W. C. Keller, V. Hesany, T. Hara, E. Bock and M. A. Donelan, 1999: Bound waves and Bragg scattering in a wind-wave tank. *J. Geophys. Res.*, **104**(C2), 3243–3263.

Plant, W. J., E. A. Terray, R. A. P. Jr. and W. C. Keller, 1994: The dependence of microwave backscatter from the sea on illuminated area: correlation times and lengths. *J. Geophys. Res.*, **99**(C5), 9705–9723.

Smith, M. J., E. M. Poulter and J. A. McGregor, 1998: Doppler radar backscatter from ring waves. *Int. J. Remote Sens.*, **19**(2), 295–305.

Sobieski, P. W., C. Craeye and L. F. Bliven, 1999: Scatterometric signatures of multivariate drop impacts on fresh and salt water surfaces. *Int. J. Remote Sens.*, **20**(11), 2149–2166.

West, J. C. and S.-J. Ja, 2002: Two-scale treatment of low-grazing-angle scattering from spilling breaker water waves. *Radio Sci.*, **37**(4), 1054, 10.1029/2001RS002517.

Worthington, A. M., 1963: *A study of splashes. Including his 1894 lecture: The splash of a drop and allied phenomena. With an introd. and notes by Keith Gordon Irwin*. New York, Macmillan.